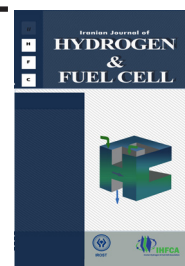Iranian Journal of Hydrogen & Fuel Cell

IJHFC

Journal homepage://ijhfc.irost.ir

Electrocatalytic oxidation of glucose on the modified carbon paste electrode with sodalite nanozeolite for fuel cell

Seyed Karim Hassaninejad-Darzi*, Fereshte Yousefi

Research Laboratory of Analytical & Organic Chemistry, Department of Chemistry, Faculty of Science, Babol University of Technology, Shariati Av., Babol, Iran. Postal Code: 47148-71167.

Article Information

Abstract

In this study, a sodalite nanozeolite was synthesized and characterized by X-ray diffraction (XRD) and scanning electronic microscopy (SEM). Following the morphology evolution of the sodalite nanozeolite in SEM images illustrated the formation of a spherical particle with a size between 60 and 80 nm. Then, a carbon paste electrode (CPE) was modified by sodalite nanozeolite and Ni^{2+} ions. The electrocatalytic performance of the fabricated electrode (Ni-SOD/CPE) towards glucose oxidation were evaluated by cyclic voltammetry and chronoamperometry in 0.1 M of NaOH solution. Also, the electron transfer coefficient, the diffusion coefficient and the mean value of catalytic rate constant for glucose and redox sites of the electrode were found to be 0.813, 3.13×10^{-5} cm^2 s^{-1} and 5.34×10^6 cm^3 mol^{-1} s^{-1}, respectively. Good catalytic activity, high sensitivity, and stability, and easy preparation qualifies the modified electrode for glucose electrooxidation. The obtained data confirmed that sodalite nanozeolite at the surface of the CPE improved the catalytic efficiency of the dispersed nickel ions toward glucose oxidation. The alkaline direct glucose fuel cells operated at ambient temperature with a Ni-SOD/CPE anode created a maximum power density of 4.1 mW cm^{-2}, cathode feed 4 mL min^{-1} of 0.1 M glucose, and oxygen at 1 bar.

1. Introduction

Alkaline direct glucose fuel cells (ADGFCs) are a promising technology because they can efficiently and directly convert the chemical energy of fuels into electrical energy [1-3]. ADGFCs that directly produce electricity from glucose appear to be a potential selection for broader applications. However, studies on ADGFCs have recently reported that electrochemical oxidation is difficult because glucose is a very stable compound [4-7]. Biological fuel and chemical energy directly converted into electricity by a microbial or enzymatic fuel cell is proposed as candidate technologies for the oxidative degradation of organic

*Corresponding Author's E-mail address: hassaninejad@nit.ac.ir
Tel: +98-11-32334203

molecules and production of electricity [8]. Because glucose is an ideal renewable fuel with the theoretical energy density of 4.43 kWh kg^{-1}, extensive efforts are being made to fabricate a glucose fuel cell [9, 10].

Compared to alcohol fuels, such as methanol and ethanol, which have been widely used in direct oxidation fuel cells (DOFCs), glucose is nontoxic, non-flammable, odourless and renewable. These properties make glucose an attractive fuel for various applications, particularly for portable electronic devices [7, 10]. Despite these advantages, fuel cells using glucose are still far from achieving practical applications. Poor glucose oxidation at the anode is one of the major challenges in the development of direct glucose fuel cells [7].

Application of electrochemical methods using nonenzymatic materials for the glucose electro oxidation have several advantages compare with using an enzyme including stability, simplicity, reproducibility, inexpensive and free of oxygen limitation [11-13]. Actually, many attempts have been made for the oxidation of glucose without an enzyme, including a Pt electrode [14], Cu electrode [15], Titanate nanotube/CuxO nanocube [16], Au nanoporous [17], Au and Au-C nanoparticles [18], modified glassy carbon electrode [19, 20] and nickel electrode [21, 22]. Nickel-based anodes are commonly used in fuel cells owing to their low cost, good chemical stability, and excellent catalytic activity toward hydrogen oxidation and reforming of small hydrocarbon molecules [7].

Zeolites constitute a valuable class of advanced crystalline microporous inorganic materials with extraordinary properties making them ideal for molecular sieving, ion-exchange and shape-selective catalytic processes [23]. They have high surface areas with strongly organized microporous channel systems that exhibits an advantage compared to other classical support materials used in fuel cell technology [24, 25]. One of the most representative artificial zeolites, sodalite, is a traditional zeolite first synthesized by the hydrothermal crystallization method [26]. It has a small pore size (2.8 Å) and high ion exchange capacity and has attracted considerable attention in industry

for optical material, hydrogen storage and catalyst support [27]. It has been pointed out that zeolites have been utilized for zeolite modified electrodes (ZMEs) and applied in electrocatalysis reaction [28].

With respect to our literature survey, no sodalite nanozeolites have been utilized for the modification of a carbon paste electrode towards electrocatalytic oxidation of glucose. In this study, sodalite nanozeolite was synthesized and characterized by XRD and SEM techniques. Then, this nanozeolite was applied for the modification of CPE and Ni^{2+} ions incorporated into this electrode by immersion of the modified electrode in a 0.5 M nickel chloride solution to obtain a Ni-SOD/CPE electrode. This modified electrode was then applied for the electrocatalytic oxidation of glucose in an alkaline medium.

2. Experimental

2.1. Reagents and materials

Sodium metasilicate (Na$_2$O$_3$Si•5H$_2$O), sodium aluminate (NaAlO$_2$), sodium hydroxide, glucose, NiCl$_2$•6H$_2$O, potassium ferricyanide (K$_4$Fe(CN)$_6$) and potassium chloride were purchased from the Merck company that were of analytical reagent grade. Graphite powder and paraffin oil from the Dayjung Company (d = 0.88 g cm^{-3}) were used as the binding agent for preparing the pastes. All materials were used without any further purification. Also, all solutions were prepared with deionized water.

2.2. Synthesis of sodalite nanozeolite

Sodalite nanozeolite was synthesized by the hydrothermal crystallization method using Na$_2$O$_3$Si•5H$_2$O and NaAlO$_2$ as a silica and aluminum source, respectively. In a typical synthesis, solution A was prepared by dissolving 18.25g of Na$_2$O$_3$Si•5H$_2$O (43 % H$_2$O, 29 % Na$_2$O, 28 % SiO$_2$) in 8 mL of double distilled water at 80 °C. Also, solution B was prepared by dissolving 3.1 g NaOH in 32 mL double distilled water which is used for solving 1.84 g

of $NaAlO_2$. Then, solution A was added to solution B dropwise under vigorous stirring and aged for 1 h under stirring before hydrothermal treatment. The molar composition of the above reactant was as follows: 1.0 Al_2O_3: 3.8 SiO_2: 2.1 Na_2O: 50 H_2O [28]. The above gel was then transferred into a Teflon-lined stainless steel autoclave and heated at 100 °C for 48 h under static condition. After this procedure, the product was separated by centrifuge (10000 rpm), washed several times with double distilled water until the pH value of the solution was about 9.0 and dried overnight at 90 °C.

2.3. Apparatus

The electrochemical experiments were performed at room temperature using a SAMA500 potantiostat/galvanostat electrochemical analysis system (Iran, Isfahan) with a voltammetry cell in a three electrode configuration. The Ag|AgCl|KCl (3 M) and platinum wire were used as reference and auxiliary electrodes, respectively. A bare CPE and modified CPE with sodalite nanozeolite (SOD/CPE) were used as working electrodes.

2.4. Preparation of the working electrode

Typically, diethyl ether was added to a mixture of 0.03g sodalite nanozeolites and 0.17g of graphite powder. After hand mixing with a mortar and pestle, the solvent was evaporated by stirring. Then, paraffin oil (35 wt%) was blended with the mixture in a mortar by hand mixing for 30 min until a uniformly wetted paste was obtained. This paste was packed into the end of a glass tube (ca. 0.35 cm i.d. and 10 cm long) and a copper wire was utilized for the electrical contact. A new surface was achieved by pushing an excess of the paste out of the tube and polishing with a weighing paper. For comparison, the unmodified CPE (bare CPE) was prepared in the same way without sodalite nanozeolites.

3. Results and discussion

3.1. Characterization of sodalite nanozeolite

The XRD powder pattern of synthesized sodalite nanozeolite is presented in Fig. 1. The crystallization products matched the characteristic peaks of sodalite nanozeolite reported by Treacy and Higgins [29], suggesting successful synthesis of sodalite nanozeolite with good crystallinity. The chemical formula of this nanozeolite is $Na_6[AlSiO_4]_{6.8}H_2O$ [26, 29, 30]. The
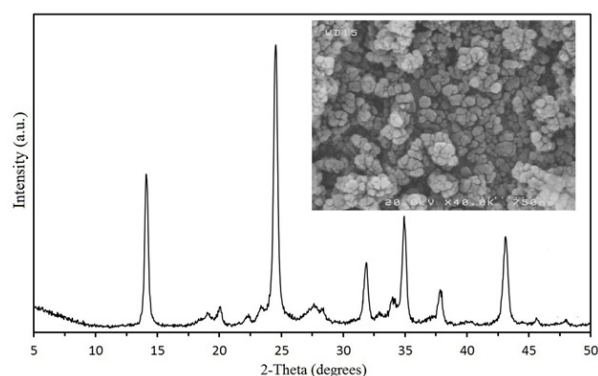

Fig. 1. The representation XRD pattern of synthesized sodalite nanozeolite. Inset show SEM image of this sample.

crystallite size (D_c) of the synthesized nanozeolite was also calculated using Debye-Scherrer equation [31]:

$$D_c = \frac{0.9\,\lambda}{\beta\,Cos\,\theta} \tag{1}$$

where λ is the wavelength of the X-ray source used in the XRD (0.15418 nm), β is the breadth of the observed diffraction line at its half-intensity maximum in radian, and θ is the main Bragg peak angle. According to the obtained results from the XRD pattern, β was 0.108 degree at $2\theta = 24.6°$. The crystallite size (D_c) of the synthesized sodalite nanozeolite obtained was 75.3 nm.

The SEM image of crystalline phase provides a useful approach for the determination of size and morphology of the obtained crystals. The SEM image in the inset of Fig. 1 illustrates synthesized sodalite nanocrystals, and indicates the formation of platelet-like nano sized particles with a size of 60–80 nm can be observed.

3.2. Electrochemistry of fabricated electrodes

Cyclic voltammetry (CV) was applied for the investigation of electrochemical properties of the unmodified CPE and modified CPE (SOD/CPE) in potassium ferricyanide ($K_4Fe(CN)_6$) solution. Fig. 2 illustrates the CVs of the electrochemical oxidation of $K_4Fe(CN)_6$ for the fabricated bare CPE and SOD/CPE electrodes in 10 mM of $K_4Fe(CN)_6$ and 0.1 M of KCl solution. As can be seen in Fig. 2, the anodic and cathodic peak currents for SOD/CPE are about 1.7-fold greater than that for the bare CPE.
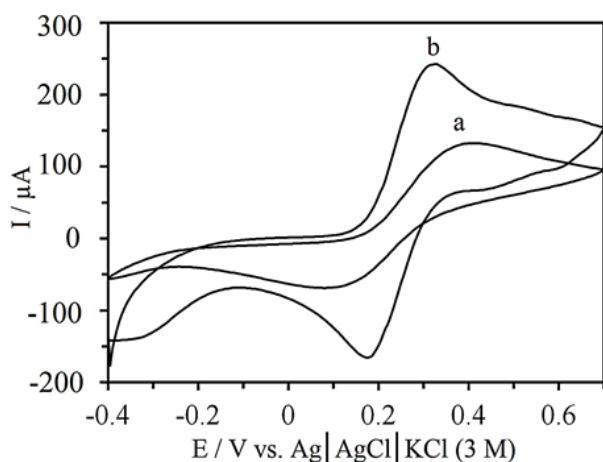

Fig. 2. The CVs of (a) bare CPE and (b) SOD/CPE in the presence of 10 mM $K_4Fe(CN)_6$ and 0.1 M KCl solution at a scan rate of 25 mV s^{-1} and pH of 7.

The experimental results show reproducible anodic and cathodic peaks ascribed to a $Fe(CN)_6^{3-}/Fe(CN)_6^{4-}$ redox couple at slow scan rates at the surface of the SOD/CPE. This is a quasi-reversible system because the peak separation potential, ΔE_p ($E_{pa}-E_{pc}$), is equal to 140 mV and is greater than 59 mV expected for a reversible system. The ΔE_p at the surface of the bare CPE was found to be 320 mV, indicating an irreversible electron transfer process.

3.3. Electrocatalytic oxidation of glucose at the surface of Ni–SOD/CPE

The CVs of a bare CPE and a SOD/CPE in 0.1 M NaOH solution at the potential range of 0.2 to 0.7 V vs. Ag|AgCl|KCl (3 M) and the potential sweep rate of 25 mV s^{-1} were recorded (data not shown). The obtained results showed that no current could be achieved with these electrodes. In order to incorporate Ni^{2+} ions at the surface of the CPE and SOD/CPE electrodes, these electrodes were immersed in a well-stirred aqueous solution of 0.5 M NiCl$_2$ at an open circuit for 20 min at 150 rpm and then washed completely with distilled water to remove the surface adsorbed species.

Figs. 3a and 3c display the CVs of Ni/CPE and Ni-SOD/CPE electrodes (CPE and SOD/CPE immersed in the 0.5 M NiCl$_2$) in 0.1 M NaOH solution and a sweep rate of 25 mV s^{-1}, respectively. It can be deduced that the electrochemical behavior of the Ni-SOD/CPE modified electrode in alkaline solution is similar to that of the Ni anode [23, 32]. These redox
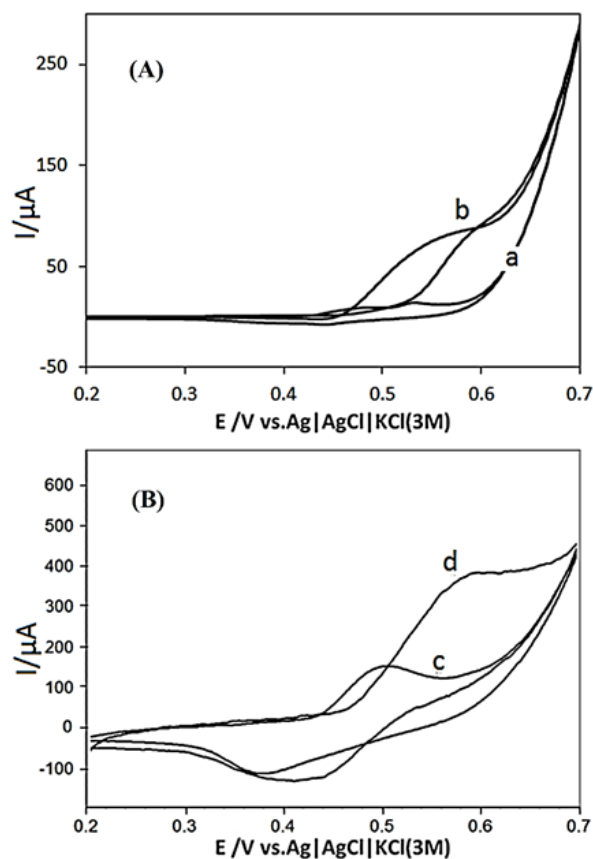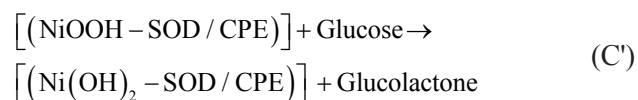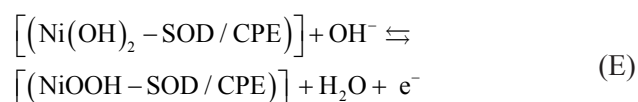

Fig. 3. (A) The CVs of the Ni/CPE (a) in the absence and (b) presence of 0.01 M glucose. (B) The CVs of the Ni-SOD/CPE (c) in the absence and (d) presence of 0.01 M glucose in 0.1 M NaOH at scan rate of 25 mV s^{-1}.

waves are ascribed to the oxidation of Ni(OH)$_2$ at the SOD/electrolyte interface to NiOOH and a reduction of NiOOH to Ni(OH)$_2$ with a peak potential of 0.50 and 0.39 V vs. Ag|AgCl|KCl (3 M), respectively [23, 32].

Comparing Fig. 3a and 3c, it can be seen that the presence of sodalite nanozeolite in the electrode construction improved the accumulation of nickel species on the surface of the fabricated electrode. After stabilization of the nickel species on the surface of the electrodes, the anodic and cathodic peak currents for the Ni-SOD/CPE were much greater than those of the Ni/CPE. As can be seen in Fig. 3a and 3c, the peak current of Ni(OH)$_2$ oxidation at the surface of Ni-SOD/CPE is about 7-fold greater than that at the Ni/CPE. These observations clearly describe the role of the sodalite nanozeolite on the enhancement of oxidation currents. The variation between the voltammetric behaviors of Ni^{2+} ions in the Ni/CPE and Ni-SOD/CPE electrodes appeared to be due to the different coordination and mobility of Ni^{2+} ions in various site of sodalite nanozeolite and graphite [23, 33].

The electrochemical oxidation of glucose was investigated at the surface of the Ni/CPE and Ni-SOD/CPE in 0.1 M NaOH solution. Figs. 3b and 3d display the CVs for electrocatalytic oxidation of the glucose in the surface of Ni/CPE and Ni-SOD/CPE electrodes in 0.1 M NaOH solution and 0.01 M glucose at a scan rate of 25 mV s^{-1}, respectively. In the presence of glucose, an increase in the current was observed at the surface of Ni-SOD/CPE (see Fig. 3d) but no significant variation in the current intensity was observed at the surface of Ni/CPE (see Fig. 3b). Comparison of curves b and d in Fig. 3 demonstrates that incorporation of sodalite nanozeolite onto a carbon paste electrode enhances the electrochemical signal of glucose oxidation. Also, oxidation of glucose gives rise to a typical electrocatalytic response, with an increase in the anodic peak current and a decrease in the cathodic peak current. The oxidation potential of glucose was observed at ca. 0.59 V which was more positive than the potential observed for Ni^{2+} to Ni^{3+} transition at the Ni-SOD/CPE in the absence of glucose (i.e. 0.50 V).

According to the literature [34], the oxidation of glucose to gluconolactone can be catalyzed by the NiOOH/Ni(OH)$_2$ redox couple in the alkaline medium. When glucose diffuses from the bulk solution to the surface of an electrode it is quickly oxidized to gluconolactone by the NiOOH species on the electrode surface [35, 36]. Therefore, the amount of NiOOH species decreases due to its chemical reaction with glucose. Simply, the electrocatalytic oxidation mechanism of glucose at Ni- SOD/CPE can be described by the following equation (i.e. EC′ mechanism) which is the basis for the fabrication of a nonenzymatic sensor for electrooxidation of glucose:

$$\left[\left(Ni(OH)_2 - SOD / CPE\right)\right] + OH^- \leftrightarrows$$
$$\left[\left(NiOOH - SOD / CPE\right)\right] + H_2O + e^- \qquad (E)$$

$$\left[\left(NiOOH - SOD / CPE\right)\right] + Glucose \rightarrow$$
$$\left[\left(Ni(OH)_2 - SOD / CPE\right)\right] + Glucolactone \qquad (C')$$

In order to obtain information about the rate determining step, a Tafel plot was illustrated for the Ni-SOD/CPE using the data derived from the raising part of the current-voltage curve for electrocatalytic oxidation of glucose. Fig. 4 illustrates the plot of log I_p vs. E_p in the presence of 0.01 M glucose at a scan rate of 10 mV s^{-1} in 0.1 M NaOH solution on the surface of the Ni-SOD/CPE. The Tafel slope was found to be 6.3212 V decade^{-1}, which indicates that the transfer coefficient (α) for madiated electrooxidation of glucose is about 0.813.

The effect of glucose concentrations on the CV of the Ni-SOD/CPE was investigated to discover the mechanism of electrochemical oxidation of the glucose on the surface of the modified electrode (see Fig. 5). As shown in Fig. 5, when concentration of glucose increases, the anodic current increases remarkably; moreover the cathodic current decreases and disappears in a high concentration of glucose [28, 37, 38].

The dependence of the glucose electrooxidation current on the scan rate of the potential (υ) under optimal conditions was studied in the range of 0.010–0.400 Vs^{-1}
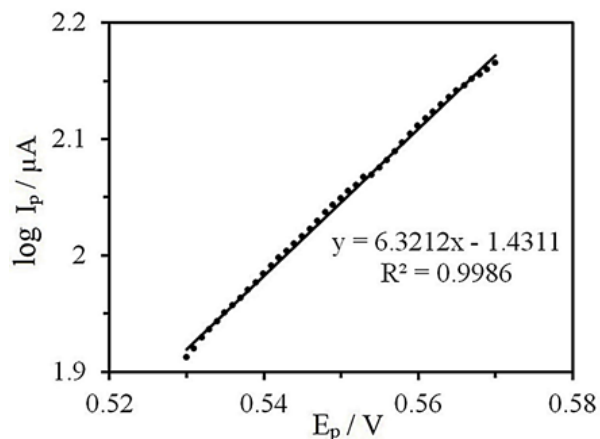
Fig. 4. The Tafel plot derived from the rising part of the CV recorded for the electrocatalytic oxidation of 0.01 M glucose at a scan rate of 10 mV s⁻¹ at the surface of Ni-SOD/CPE in 0.1 M NaOH solution.

for the Ni-SOD/CPE. Fig. 6a shows the CVs of this electrode in the presence of 0.006 M glucose in 0.1 M NaOH. Increases in the peak current with the υ can be considered for adsorption or diffusion control of the process. Fig. 6b shows the plot of anodic current density (I_{pa}) versus scan rate (υ), while Fig. 6c displays the plot of I_{pa} versus square root of scan rate ($\upsilon^{1/2}$). As can be seen, the plot of I_{pa} versus $\upsilon^{1/2}$ was found to be linear, while the plot of I_{pa} against υ did not show a linear curve. From this observation, it can be realized that this process is a diffusion-controlled process rather than a surface-controlled process

[39]. From a theoretical point, a slope of 0.5 or 1.0 is expected for the plot of log I_{pa} vs. log υ under diffusion or adsorption control, respectively [32]. Fig. 6d shows a linear dependence between log I_{pa} and log υ at the surface of the Ni-SOD/CPE for oxidation of glucose. From the linear section, the slope of 0.313 was found which is near the theoretically predicted value of 0.5 for a purely diffusion-controlled current. However, the contribution of kinetic limitation to the overall process causes the small alteration of the theoretical value [40]. Also, the characteristic shape of an EC′ mechanism was detected in a plot of the scan rate normalized current ($I_{pa}/\upsilon^{1/2}$) vs. the logarithm scan rate (log υ) (see Fig. 6e) showing that the electrode reaction is coupled with an irreversible follow up chemical step [41].

3.4. Chronoamperometric studies

We performed some chronoamperometric measurements to evaluate the electrocatalytic performance of the Ni-SOD/CPE for glucose oxidation. The current–time curves of the Ni/CPE and Ni-SOD/CPE were recorded for the electrooxidation of 0.005 M glucose (data not shown). The currents of glucose oxidation decayed rapidly on the Ni/CPE; however, the currents of glucose oxidation decayed slowly on the surface of the Ni-SOD/CPE and the initial current of glucose oxidation on the
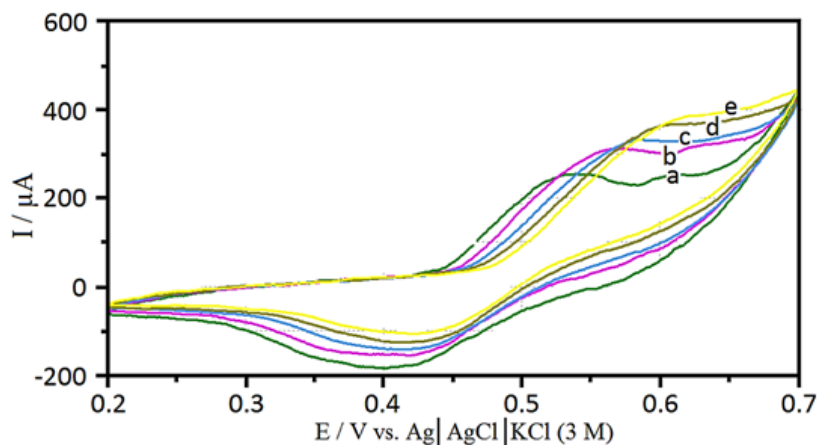

Fig. 5. Current-potential curves from Ni-SOD/CPE in the electrocatalytic oxidation of glucose at the scan rate of 25 mV s⁻¹ in 0.1 M NaOH solution and glucose concentration of (a) 0.02, (b) 0.04, (c) 0.06, (d) 0.08 and (e) 0.1 M.
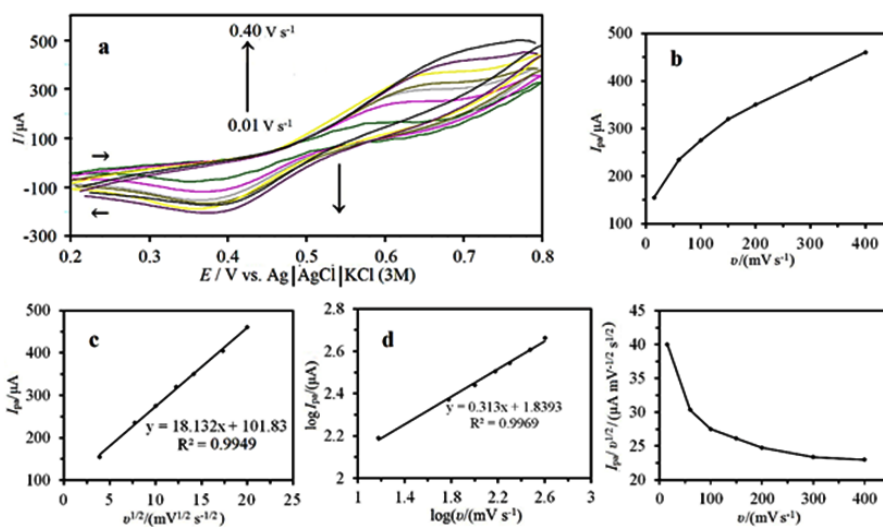
Fig. 6. (a) The CVs of the Ni-SOD/CPE in the presence of 0.006 M glucose in 0.1 M NaOH at various scan rates from 0.01, 0.06, 0.0100, 0.15, 0.2, 0.3 and 0.40 V s⁻¹. (b) Variation of I_{pa} vs. v, (c) Variation of I_{pa} vs. $v^{1/2}$, (d) The plot of log I_{pa} vs. log v and (e) The plot of $I_{pa}/v^{1/2}$ vs. v.

Ni-SOD/CPE was higher than that on the Ni/CPE. These results indicate that a greater number of active sites are available for oxidation of glucose on the Ni-SOD/CPE and are in agreement with the CV results [42].

Fig. 7A illustrates double step chronoamperometric measurements at the surface of the Ni-SOD/CPE with several concentrations of glucose such as 0.0, 0.001, 0.005 and 0.01 M. The applied potential steps were 0.60 (in the first step) and 0.38 V (in the second step) vs. Ag|AgCl|KCl (3M) determined based on peak potential of the redox process at various
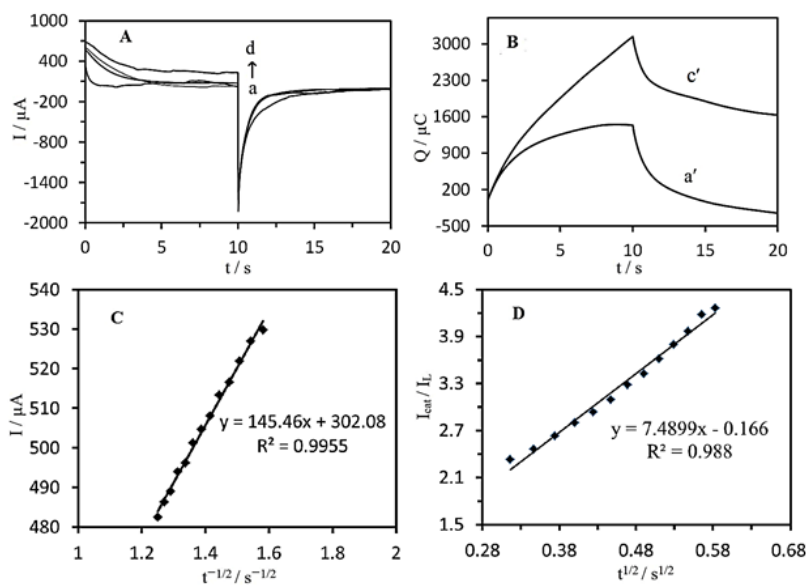
Fig. 7. (A) The double step chronoamperograms of Ni-SOD/CPE in 0.1 M NaOH solution in the a absence and presence of (b) 0.001, (c) 0.005, (d) 0.01 M of glucose (The potential steps were 0.60 and 0.38 V vs. Ag/AgCl/KCl (3 M)). (B) Charge-time curves in the absence (a′) and presence of 0.005 M glucose (c′). (C) Dependence of I on $t^{-1/2}$, derived from the data of chronoamperogram (b). (D) Dependence of I_{cat}/I_L on $t^{1/2}$, derived from the data of chronoamperogram (c).

concentrations of glucose. It was found that the observed current from chronoamperograms was in good agreement with the observed current from the CV experiments, and the current increases as the glucose concentration increases (curves b–d). This result supports our conclusion about the catalytic role of NiOOH for oxidation of glucose that oxidation starts directly after the formation of the first amount of NiOOH on the surface of electrode [43].

The forward and backward potential step chronoamperometry of the Ni-SOD/CPE electrode in the blank solution showed an almost symmetrical chronoamperograms, which demonstrates that almost equivalent charges were consumed for the oxidation and reduction of surface confined $Ni(OH)_2$/NiOOH sites. However in the presence of glucose, the charge value associated with the forward chronoamperometry is greater than that observed for the backward chronoamperometry (see Fig. 7B).

From the chronoamperometric study, the diffusion coefficient of the glucose was determined in aqueous solution by using Cottrell equation as below [44]:

$$I = nFACD^{1/2}.\pi^{-1/2}.t^{-1/2} \qquad (2)$$

where F is the faraday number, A is the area of the electrode, C is the known concentration of glucose and D is the apparent diffusion coefficient. Fig. 7C demonstrates experimental plots of I vs. $t^{-1/2}$ for 1.0 mM glucose at the surface of the Ni-SOD/CPE. The same curves were plotted for all concentrations and then the slopes of the resulting straight lines were plotted vs. the glucose concentration. From the slope of the resulting plots and using the Cottrell equation, the mean value of D was calculated to be 3.13×10^{-5} $cm^2 s^{-1}$ (with n=2, F=96485 C mol^{-1} and A=0.096 cm^2) [45].

Chronoamperometry can be used for the evaluation of the catalytic rate constant (k_{cat}) of the electrocatalytic oxidation of glucose on the active sites of the modified electrode according to the following equation [46]:

$$\frac{I_{cat}}{I_L} = \pi^{1/2}\left(k_{cat}C_o t\right)^{1/2} \qquad (3)$$

where, I_{cat} and I_L are the currents in the presence and absence of glucose, respectively. The symbol k_{cat} is the catalytic rate constant (cm^3 mol^{-1} s^{-1}), C_0 is the bulk concentration of glucose (mol cm^{-3}) and t is the elapsed time (s). Fig. 7D displays the experimental plots I_{cat}/I_L versus $t^{1/2}$ derived from the current in the presence of 0.005 M glucose divided to the current in the absence of glucose. From the slopes of the I_{cat}/I_L versus $t^{1/2}$ for all concentrations, the mean value of k_{cat} was calculated to be 5.34×10^6 cm^3 mol^{-1} s^{-1}. Comparison of the estimated kcat with other kcat values in the literature are presented in Table 1 [12, 45, 47, 48, 50]. This table also shows that a lower over potential of glucose oxidation was obtained at the surface of the Ni-SOD/CPE as compared with that at some of the previously reported electrodes [12, 47, 48, 50].

Steady state polarization studies were conducted for alkaline direct glucose fuel cells (ADGFCs) at the surface of the Ni-SOD/CPE as anode catalyst at room temperature. Figure 8 (all previous sentences used Fig. instead of Figure, be consistent) shows steady state performance curves for ADGFCs with aqueous 1 M NaOH containing 0.1 M glucose and oxygen as fuel and oxidant, respectively. This cell shows the peak power density of 4.1 mW cm^{-2}.
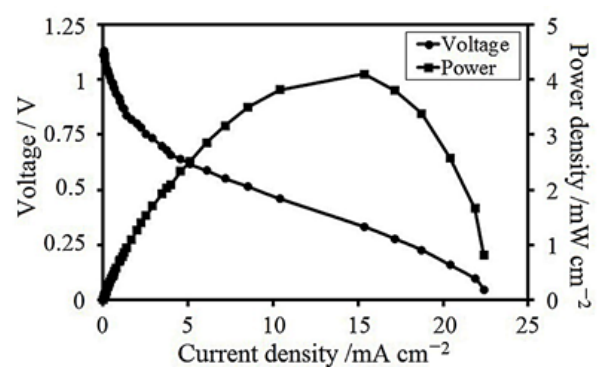

Fig. 8. Steady state performance curves for ADGFCs (glucose and oxygen) at the surface of Ni-SOD/CPE as anode catalysts at room temperature.

4. Conclusions

In summary, we synthesized an aluminosilicate

Table 1 Comparison of the catalytic rate constant and oxidation potential of Ni-SOD/CPE for the glucose oxidation with some of the previously reported work in 0.1 M NaOH.

Electrode	kcat (cm³ mol⁻¹ s⁻¹)	Applied potential (V) vs. Ag/AgCl/ KCl (3 M)	Ref.
Cu nanocluster/MWCNT/GCE	-------	0.65	[11]
Ni(II)–Qu–MWCNT–IL–PE	1.91×10^6	0.48	[12]
Dimethylglycoxime/Cu (DMG-CuNPs)	-------	0.69	[15]
Cu-based metal organic framework	1.554×10^7	0.59	[45]
Cu–Co–Ni/carbon nanofibers/GCE	2.2×10^6	0.55	[47]
Ni/poly (1-naphthylamine)/CPE	229	-------	[48]
Ni/carbon nanofiber paste electrode	-------	0.60	[49]
Ni-POAP/CPE	1.8×10^6	-------	[50]
Ni-SOD/CPE	5.34×10^6	0.59	This work

nanozeolite type sodalite and characterized it by XRD and SEM techniques. Results from the XRD pattern and SEM images demonstrated that the synthesized sodalite nanozeolite was a semi spherical particle with a size of 60-80 nm. Then, a novel modified CPE was developed by this nanozeolite. This new modified electrode (Ni-SOD/CPE) was utilized toward the electrocatalytic oxidation of glucose in alkaline solution, and the results were examined by cyclic voltammetry and Chronoamperometry. The modified electrode enhanced the oxidation of glucose through a decrease in over potential of glucose oxidation and overcame the low kinetic of reaction in alkaline solution. Results specified that the NiOOH species formed during the oxidation of SOD/CPE was found to be a good catalyst for oxidation of glucose. It can be stated from the obtained results that this non-noble catalyst, Ni-SOD/CPE, has some advantages such as low cost and stability, ease of preparation and regeneration, stable response and very low ohmic resistance in fuel cell. If not, then the sentence needs to be changed into two sentences to be clear.

5. References

[1] Lu S.J., Ji S.B., Liu J.C., Li H. and Li W.S., "Photoelectrocatalytic oxidation of glucose at a ruthenium complex modified titanium dioxide electrode promoted by uric acid and ascorbic acid for photoelectrochemical fuel cells", J. Power Sources, 2015, 273: 142.

[2] Mclntosh S. and Gorte R.J., "Direct Hydrocarbon Solid Oxide Fuel Cells", Chem. Rev., 2004, 104: 4845.

[3] Kwon B.W., Hu S., He Q., Marin-Flores O.G., Oh C.H., Yoon S.P., Kim J., Breit J., Scudiero L., Norton M.G. and Ha S., "Nickel-based anode with microstructured molybdenum dioxide internal reformer for liquid hydrocarbon-fueled solid oxide fuel cells", Appl. Catal. B: Environ., 2015, 179: 439.

[4] Fujiwara N., Yamazaki S.-I., Siroma Z., Ioroi T., Senoh H. and Yasuda K., "Nonenzymatic glucose fuel cells with an anion exchange membrane as an electrolyte", Electrochem. Commun., 2009, 11: 390.

[5] An L., Zhao T.S., Shen S.Y., Wu Q.X. and Chen R., "Alkaline direct oxidation fuel cell with non-platinum catalysts capable of converting glucose to electricity at high power output", J. Power Sources, 2011, 196: 186.

[6] Yu E.H., Wang X., Krewer U., Li L. and Scott K., "Direct oxidation alkaline fuel cells: from materials to systems", Energy Environ. Sci., 2012, 5: 5668.

[7] Li L., Scott K. and Yu E.H., "A direct glucose alkaline fuel cell using MnO$_2$-carbon nanocomposite supported gold catalyst for anode glucose oxidation", J. Power Sources, 2013, 221: 1.

[8] Davis F. and Higson S.P.J., "Biofuel cells-Recent advances and applications", Biosens. Bioelectron., 2007, 22: 1224.

[9] Elouarzaki K., Haddad R., Holzinger M., Goff A.L., Thery J., Cosnier S., "MWCNT-supported phthalocyanine cobalt as air-breathing cathodic catalyst in glucose/O$_2$ fuel cells", J. Power Sources, 2014, 255: 24.

[10] Ishimoto T., Hamatake Y., Kazuno H., Kishida T. and Koyama M., "Theoretical study of support effect of Au catalyst for glucose oxidation of alkaline fuel cell Anode", Appl. Surf. Sci., 2015, 324: 76.

[11] Kang X., Mai Z., Zou X., Cai P. and Mo J., "A sensitive nonenzymatic glucose sensor in alkaline media with a copper nanocluster/multiwall carbon nanotube-modified glassy carbon electrode", Anal. Biochem., 2007, 363: 143.

[12] Zheng L., Zhang J. and Song J., "Ni(II)–quercetin complex modified multiwall carbon nanotube ionic liquid paste electrode and its electrocatalytic activity toward the oxidation of glucose", Electrochim. Acta, 2009, 54: 4559.

[13] Park S., Boo H. and Chung T.D., "Electrochemical non-enzymatic glucose sensors", Anal. Chim. Acta, 2006, 556: 46.

[14] Rong L.Q., Yang C., Qian Q.Y. and Xi X.H., "Study of the nonenzymatic glucose sensor based on highly dispersed Pt nanoparticles supported on carbon nanotubes", Talanta, 2007, 72: 819.

[15] Xu Q., Zhao Y., Xu J.Z. and Zhu J.J., "Preparation of functionalized copper nanoparticles and fabrication of a glucose sensor", Sensor, Actuat. B-Chem., 2006, 114: 379.

[16] Shi H., Zhou S., Feng X., Huang H., Guo Y. and Song W., "Titanate nanotube forest/CuxO nanocube hybrid for glucose electro-oxidation and determination", Sensor Actuat. B-Chem., 2014, 190: 389.

[17] Qiu H. and Huang X., "Effects of Pt decoration on the electrocatalytic activity of nanoporous gold electrode toward glucose and its potential application for constructing a nonenzymatic glucose sensor", J. Electroanal. Chem., 2010, 643: 39.

[18] Karczmarczyk A., Celebanska A., Nogala W., Sashuk V., Chernyaeva O. and Opallo M., "Electrocatalytic glucose oxidation at gold and gold-carbon nanoparticulate film prepared from oppositely charged nanoparticles", Electrochim. Acta, 2014, 117: 211.

[19] Ghonim A.M., El-Anadouli B.E. and Saleh M.M., "Electrocatalytic glucose oxidation on electrochemically oxidized glassy carbon modified with nickel oxide nanoparticles", Electrochim. Acta, 2013, 114: 713.

[20] El-Refaei S.M., Awad M.I., El-Anadouli B.E. and Saleh M.M., "Electrocatalytic glucose oxidation at binary catalyst of nickel and manganese oxides nanoparticles modified glassy carbon electrode: Optimization of the loading level and order of deposition", Electrochim. Acta, 2013, 92: 460.

[21] Galindo R., Gutierrez S., Menendez N. and Herrasti P., "Catalytic properties of nickel ferrites for oxidation of glucose, β-nicotiamide adenine dinucleotide (NADH) and methanol", J. Alloys Compd., 2014, 586: S511.

[22] Velarde A.M., Bartl P., Nieen T.E.W. and Hoelderich W.F., "Hydrogen peroxide oxidation of d-glucose with titanium-containing zeolites as catalysts", J. Mol. Catal. A-Chem., 2000, 157: 225.

[23] Samadi-Maybodi A., Hassani Nejad-Darzi S.K., Ganjali M.R. and Ilkhani H., "Application of nickel phosphate nanoparticles and VSB-5 in the modification of carbon paste electrode for electrocatalytic oxidation of methanol", J. Solid State Electrochem., 2013, 17: 2043.

[24] Hassaninejad–Darzi S.K. and Rahimnejad M., "Electrocatalytic oxidation of methanol by ZSM-5 nanozeolite modified carbon paste electrode in alkaline medium", J. Iran. Chem. Soc., 2014, 11: 1047

[25] Li L., Li W., Sun C. and Li L., "Fabrication of carbon paste electrode containing 1:12 phosphomolybdic anions encapsulated in modified mesoporous molecular sieve MCM-41 and its electrochemistry", Electroanalysis, 2002, 14: 368.

[26] Felsche J., Luger S. and Baerlocher C., "Crystal structures of the hydro-sodalite $Na_6[AlSiO_4]_{6.8}H_2O$ and of the anhydrous sodalite $Na_6[AlSiO_4]_6$", Zeolites, 1986, 6: 367.

[27] Ogura M., Morozumi K., Elangovan S.P. and Okubo T., "Potassium-doped sodalite: A tectoaluminosilicate for the catalytic material towards continuous combustion of carbonaceous matters", Appl. Catal. B-Environ., 2008, 77: 294.

[28] Rahimnejad M., Hassaninejad-Darzi S.K. and Pourali S.M., "Preparation of template-free sodalite nanozeolite-chitosan-modified carbon paste electrode for electrocatalytic oxidation of ethanol", J. Iran. Chem. Soc., 2015, 12: 413.

[29] Treacy M.M.J. and Higgins J.B., "Collection of simulated XRD powder patterns for zeolites, published on behalf of the structure commission of the international zeolite association", 5th revised edition, Elsevier, Amsterdam, 2007.

[30] Arieli D., Vaughan D.E.W. and Goldfarb D., "New synthesis and insight into the structure of blue ultramarine pigments", J. Am. Chem. Soc., 2004, 126: 5776.

[31] Klug H.P. and Alexander L.E., "X-ray Diffraction Procedures", second ed., John Wiley & Sons, New York, 1964.

[32] Fleischmann M., Korinek K. and Pletcher D., "The oxidation of organic compounds at a nickel anode in alkaline solution", J. Electroanal. Chem., 1971, 31: 39.

[33] Mojovic Z., Mentus S. and Krstic I., "Thin layer of Ni-modified 13X zeolite on glassy carbon support as an electrode material in aqueous solutions", Russ. J. Phys. Chem. A, 2007, 81: 1452.

[34] Lu L.M., Zhang L., Qu F.L., Lua H.X., Zhang X.B., Wu Z.S., Huan S.Y., Wang Q.A., Shen G.L. and Yu R.Q., "A nano-Ni based ultrasensitive nonenzymatic electrochemical sensor for glucose: enhancing sensitivity through a nanowire array strategy", Biosens. Bioelectron., 2009, 25: 218.

[35] Hassaninejad–Darzi S.K., "A novel, effective and low cost catalyst for formaldehyde electrooxidation based on nickel ions dispersed onto chitosan-modified carbon paste electrode for fuel cell", J. Electroceram., 2014, 33: 252.

[36] Lim S.H., Wei J., Lin J., Li Q. and You J.K., "A glucose biosensor based on electrodeposition of palladium nanoparticles and glucose oxidase onto Nafion-solubilized carbon nanotube electrode", Biosens. Bioelectron., 2005, 20: 2341.

[37] Yi Q., Zhang J., Huang W. and Liu X., "Electrocatalytic oxidation of cyclohexanol on a nickel oxyhydroxide modified nickel electrode in alkaline solutions", Catal. Commun., 2007, 8: 1017.

[38] Prokofev Y.Y., and Gordina N.E., "Preparation of granulated LTA and SOD zeolites from mechanically activated mixtures of metakaolin and sodium hydroxide", Appl. Clay Sci., 2014, 101: 44.

[39] Bard A.J. and Faulkner L.R., Electrochemical methods: fundamentals and applications, Wiley, New York, 2001.

[40] Velazquez-Palenzuela A., Centellas F., Garrido J.A., Arias C., Rodriguez R.M., Brillas E. and Cabot P.L., "Kinetic analysis of carbon monoxide and methanol oxidation on high performance carbon-supported Pt-Ru electrocatalyst for direct methanol fuel cells", J. Power Sources, 2011, 196: 3503.

[41] Gosser D.K.J., Cyclic voltammetry-simulation and analysis of reaction mechanism, Wiley, New York, 1993.

[42] Dimos M.M. and Blanchard G.J., "Evaluating the role of catalyst morphology on electro-catalytic methanol and ethanol oxidation", J. Phys. Chem. C, 2010, 114: 6019.

[43] El-Shafei A.A., "Electrocatalytic oxidation of methanol at a nickel hydroxide/glassy carbon modified electrode in alkaline medium", J. Electroanal. Chem., 1999, 471: 89.

[44] Greef R., Peat R., Peter L.M., Pletcher D. and Robinson J., Instrumental methods in electrochemistry, Chichster, Ellis Horwood, 1990.

[45] Wei C., Li X., Xu F., Tan H., Li Z., Sun L. and Song Y., "Metal organic framework-derived anthill-like Cu@ carbon nanocomposites for nonenzymatic glucose sensor", Anal. Methods, 2014, 6: 1550.

[46] Vilas-Boas M., Freire C., Castro B.D. and Hillman A.R., "Electrochemical characterization of a novel salen-type modified electrode", J. Phys. Chem. B, 1998, 102: 8533.

[47] Liu H., Lu X., Xiao D., Zhou M., Xu D., Sunb L. and Song Y., "Hierarchical Cu–Co–Ni nanostructures electrodeposited on carbon nanofiber modified glassy carbon electrode: application to glucose detection", Anal. Methods, 2013, 5: 6360.

[48] Ojani R., Raoof J.B. and Salmany-Afagh P., "Electrocatalytic oxidation of some carbohydrates by poly(1-naphthylamine)/nickel modified carbon paste electrode", J. Electroanal. Chem., 2004, 571: 1.

[49] Liu Y., Teng H., Hou H. and You T., "Nonenzymatic glucose sensor based on renewable electrospun Ni nanoparticle-loaded carbon nanofiber paste electrode", Biosens. Bioelectron., 2009, 24: 3329.

[50] Ojani R., Raoof J.B. and Fathi S., "Electrocatalytic oxidation of some carbohydrates by nickel/poly (o-aminophenol) modified carbon paste electrode", Electroanalysis, 2008, 20: 1825.